Computation of thermodynamic properties in the continuous fractional component Monte Carlo Gibbs ensemble

Poursaeidesfahani, Ali; Rahbari, A.; Torres-Knoop, Ariana; Dubbeldam, David; Vlugt, Thijs J H

DOI
10.1080/08927022.2016.1244607

Publication date
2017

Document Version
Accepted author manuscript

Published in
Molecular Simulation

Computation of Thermodynamic Properties in the Continuous Fractional Component Monte Carlo Gibbs Ensemble

Ali Poursaeidesfahani,[†] Ahmadreza Rahbari,[†] Ariana Torres-Knoop,[‡] David Dubbeldam,[‡] and Thijs J.H. Vlugt[*,†]

Engineering Thermodynamics, Process & Energy Department, Faculty of Mechanical, Maritime and Materials Engineering, Delft University of Technology, Leeghwaterstraat 39, 2628CB, Delft, The Netherlands, and Van't Hoff Institute for Molecular Sciences, University of Amsterdam, Science Park 904, 1098XH Amsterdam, The Netherlands

E-mail: t.j.h.vlugt@tudelft.nl

Abstract

It is shown that ensemble averages computed in the Gibbs Ensemble with Continuous Fractional Component Monte Carlo (CFCMC GE) are different from those computed in the conventional Gibbs Ensemble (GE). However, it is possible to compute averages corresponding to the conventional GE while performing simulations in the CFCMC GE. In this way, one can benefit from the nice features of CFCMC GE (e.g. more efficient particle exchange) and at the same time compute the ensemble averages that correspond to the conventional GE. As a case study, the equilibrium pressure and densities of the systems of 256 and 512 LJ particles at different reduced

[*]To whom correspondence should be addressed
[†]Delft University of Technology
[‡]Van't Hoff Institute for Molecular Sciences

temperatures (T =0.7, 0.8, 0.95) are computed in the conventional GE and CFCMC GE. The validity of the expressions derived for computation of the thermodynamic pressure and densities corresponding to the conventional GE and computed in the CFCMC GE is examined numerically. The thermodynamic pressure in the conventional GE and CFCMC GE typically differs by at most 3%. It is shown that a very good estimate of the average pressure and densities corresponding to the conventional GE can be obtained by performing simulation in CFCMC GE and ignoring the contributions of the fractional molecule. It is also shown that the fractional molecule does not have an influence on the structure of the liquid, even for very small system sizes (e.g. 40 particles). The approach used here to compute the equilibrium pressure and densities of the conventional GE using the CFCMC GE can be easily extended to other thermodynamic properties and other ensembles.

Keywords: Continuous Fractional Component Monte Carlo, Thermodynamic Properties, Gibbs Ensemble, Vapor-Liquid Equilbria.

Introduction

Coexistence properties at Vapor-Liquid Equilbria (VLE) are crucial to design many industrial processes.[1–3] Molecular simulations using Monte Carlo algorithms are widely applied to provide information regarding the thermodynamic properties of coexisting phases.[4–6] Since the introduction of Gibbs Ensemble (GE) in 1980s by Panagiotopoulos,[7–9] simulations in this ensemble are frequently used to study Vapor-Liquid Equilbria of pure components and mixtures.[10–14] Other methods such as histogram reweighting in the grand-canonical ensemble[15,16] can be more efficient to study VLE. However, since the GE is convenient and sufficiently accurate, it is still widely used for simulating phase coexistence of pure components and mixtures.[13,14]

Similar to simulations in the grand-canonical ensemble, GE simulations rely on sufficiently large acceptance probabilities for particle exchanges between the simulation boxes. However, the acceptance probability for particle exchange can be very low when molecules are large or when densities are high (e.g. adsorption close to saturation loading, or liquid phases at low temperatures),[17] even when advanced techniques like Configurational-bias Monte Carlo are used. When the acceptance probability for insertion/deletion is low, it is not straightforward to verify if the two phases have reached equilibrium and that the chemical potentials of a certain component are equal in the simulation boxes. In this case, one should separately check the conditions for chemical equilibrium (equality of pressures, chemical potentials, and temperatures for all components in the two phases). The so-called expanded ensemble methods are among possible solutions to overcome this problem.[18–20] The Continuous Fractional Component Monte Carlo (CFCMC), recently introduced by Shi and Maginn, is one of the most commonly used expanded ensemble approaches .[21–30] Poursaeidesfahani et al. have introduced a more efficient formulation of the GE combined with the CFCMC technique.[31] In this formulation, there is only a single fractional molecule per component which can be in either one of the boxes. The chemical potential can be computed directly without any extra calculations. These authors also showed that the computed chemical potentials are

identical to those computed in conventional GE, which was validated for LJ particles and water.[31] For the simple LJ fluid, the acceptance probability for insertion/deletion of particles in CFCMC GE at a reduced temperature $T = 0.7$ is five hundred times larger than in the conventional GE.[31] Although CFCMC improves the acceptance probability of particle exchange, it rises a very important question: How should one relate the properties computed in CFCMC GE simulations to those computed in the conventional GE? As an example, when computing the density of the two phases in CFCMC GE, it is not clear a priori if one should count the fractional molecule or not.[21,22,31] In this paper, we introduce general guidelines on how to relate averages computed in the CFCMC GE to averages in the conventional GE. We consider here the computation of pressure and densities in the conventional GE and in the CFCMC GE introduced by Poursaeidesfahani et al.[31] For both conventional GE and CFCMC GE, we derive equations for thermodynamic pressure of the system. We show that the calculated thermodynamic pressures of the two simulation boxes are exactly equal, and that the thermodynamic pressure of the conventional GE and CFCMC GE are different. We also show that the structure of the liquid is not influenced by the fractional molecule. We show how the expansion of the conventional GE with the fractional molecule affects the average pressure of the two boxes, and how one can compute the pressure corresponding to the conventional GE in the CFCMC GE. The pressure is chosen because of its importance in verification of the equilibrium between the two phases.

This paper is organized as follows. In section 2, the relevant equations for computing the pressures in the conventional GE, the CFCMC GE.,[31] and the pressure corresponding to the conventional GE calculated in CFCMC GE are derived, Also, guidelines for computing averages corresponding to the conventional GE and computed in the CFCMC GE are presented. The pressures and densities of the two coexisting phases of LJ particles at various temperatures computed in the conventional GE and the CFCMC GE are presented in section 3. In this section, the influence of the fractional molecule on the structure of the two phases is also investigated. Our findings are summarized in section 4.

Methodology

In the CFCMC GE formulation introduced by Poursaeidesfahani et al.,[31] there is only a single fractional molecule per component which is distinguishable from the whole molecules. In the case of LJ pair interactions, the LJ interactions of the fractional molecule are scaled according to:[22]

$$u_{\mathrm{LJ}}(r,\lambda) = \lambda 4\varepsilon \left(\frac{1}{\left[\frac{1}{2}(1-\lambda)^2 + \left(\frac{r}{\sigma}\right)^6\right]^2} - \frac{1}{\left[\frac{1}{2}(1-\lambda)^2 + \left(\frac{r}{\sigma}\right)^6\right]} \right) \tag{1}$$

where λ is the scaling parameter with $\lambda \in \langle 0,1\rangle$. The partition function of this system is given by:[31]

$$\begin{aligned} Q_{\mathrm{CFCMC}} =& \frac{1}{\Lambda^{3(N_T+1)}\,(N_T)!} \sum_{i=1}^{2} \sum_{N_1=0}^{N_T} \int_0^1 d\lambda \int_0^{V_T} dV_1 {V_1}^{N_1+\delta_{i,1}} (V_T - V_1)^{N_T-N_1+\delta_{i,2}} \frac{(N_T)!}{(N_1)!\,(N_T-N_1)!} \\ & \times \int ds^{N_1} \exp[-\beta U_{\mathrm{int},1}(s^{N_1}, V_1)] \int ds^{N_T-N_1} \exp[-\beta U_{\mathrm{int},2}(s^{N_T-N_1}, V_T - V_1)] \\ & \times \left(\begin{array}{l} \delta_{i,1} \int ds^1_{\mathrm{frac}} \exp[-\beta U_{\mathrm{frac},1}(s^1_{\mathrm{frac}}, s^{N_1}, \lambda, V_1)] \\ + \delta_{i,2} \int ds^2_{\mathrm{frac}} \exp[-\beta U_{\mathrm{frac},2}(s^2_{\mathrm{frac}}, s^{N_T-N_1}, \lambda, V_T - V_1)] \end{array} \right) \end{aligned} \tag{2}$$

where $\beta = 1/(k_B T)$ and Λ is the thermal wavelength. The fractional molecule can be transferred between the boxes and i indicates the box where fractional molecule is in. $U_{\mathrm{int},i}$ and $U_{\mathrm{frac},i}$ are the total internal energy of the whole molecules and the internal energy of the fractional molecule in box i, respectively. V_T is the total volume and V_1 is the volume of box 1. $\delta_{i,j}$ equals 1 when $i = j$ and zero otherwise.[31] Except for the trial moves used for the thermalization of the system and volume changes, three other trial moves are used to facilitate particle exchanges between the simulation boxes:

- Changing the scaling parameter λ with $\lambda \in \langle 0,1\rangle$.
- Swapping the fractional molecule between the boxes.

- Changing the identity of the fractional molecule with a randomly selected whole molecule in the other simulation box, while keeping the value of λ constant

These trial moves are illustrated in Fig. 1. By applying an appropriate biasing function, the first type of trial move allows for a smooth transformation of the fractional molecule from a molecule with no interactions to a molecule with full interactions with its surroundings. Swap and change trial moves are used to transfer the fractional molecule from one box to the other. The former trial move is very efficient for low values of λ and the latter is very efficient for high values of λ.[31] Using these trial moves, the value of λ can be efficiently changed from 0 to 1 and the fractional molecule can be transferred between the boxes at all values of λ. These trial moves, combined with volume-changes and particle displacements are sufficient to sample the partition function of Eq. 2. To improve the efficiency of simulations, a biasing function is added to make the observed probability distribution of the scaling parameter λ in the two boxes flat. The unbiased probability distribution of this scaling parameter is denoted by $p(\lambda, j)$. A sample FORTRAN code for this algorithm is available from Ref.[32] A detailed description of the trial moves and their acceptance rules are provided in Ref.[31]

Computation of the Pressure

In molecular simulations, the thermodynamic pressure is usually computed by averaging over the instantaneous microscopic pressures. In any NVT ensemble, the general expression for the thermodynamic pressure P is[33–35]

$$P = k_B T \left(\frac{\partial \ln Q}{\partial V} \right)_T \tag{3}$$

Considering the fact the Gibbs ensemble is a special case of the NVT ensemble, Eq. 3 is applicable to the GE and CFCMC GE. Starting from the partition function of the conventional GE and following the steps presented in the Supporting Information, the pressure in

the conventional GE is obtained by the conventional virial equation:[35,36]

$$P_{\mathrm{GE},j} = k_B T \left\langle \frac{N_j}{V_j} \right\rangle_{\mathrm{GE}} + \left\langle \frac{\sum_{a<b} f_j(r_{ab,j}) r_{ab,j}}{3V_j} \right\rangle_{\mathrm{GE}} \tag{4}$$

where $r_{ab,j}$ and $f_j(r_{ab,j})$ are the distance and the force acting between particles "a" and "b" in box "j"(assuming pair potentials). The first term on the right hand side of Eq. 4 is the ideal gas contribution and the second term is commonly known as the virial contribution.[35] The labeling of the boxes is arbitrary, therefore, the same equation is obtained for the other box. Since there is only one thermodynamic pressure for the system, the pressures of the two boxes are on average equal. In the same way, as shown in the Supporting Information, the thermodynamic pressure in the CFCMC GE is computed from:

$$P_{\mathrm{CFCMC},j} = k_B T \left(\frac{\partial \ln Q_{\mathrm{CFCMC}}}{\partial V_T} \right)_T = k_B T \left\langle \frac{N_j + \delta_{i,j}}{V_j} \right\rangle_{\mathrm{CFCMC}} + \left\langle \frac{\sum_{a<b} f_j(r_{ab,j}) r_{ab,j}}{3V_j} \right\rangle_{\mathrm{CFCMC}} \tag{5}$$

In this equation, the contribution of the fractional molecule is included in the ideal gas part and in the virial part. The thermodynamic pressures in the CFCMC GE (Eq. 5) and conventional GE (Eq. 4) are clearly not identical. As shown in the Supporting Information, it is possible to compute the pressure corresponding to the conventional GE while performing simulations in the CFCMC GE:

$$P^*_{\mathrm{GE},j} = k_B T \frac{\left\langle \delta_{\lambda=0,i=j} \frac{N_j}{V_j^2} \right\rangle_{\mathrm{CFCMC}}}{\left\langle \delta_{\lambda=0,i=j} \frac{1}{V_j} \right\rangle_{\mathrm{CFCMC}}} + \frac{\left\langle \delta_{\lambda=0,i=j} \frac{\sum_{a<b} f_j(r_{ab,j}) r_{ab,j}}{3V_j^2} \right\rangle_{\mathrm{CFCMC}}}{\left\langle \delta_{\lambda=0,i=j} \frac{1}{V_j} \right\rangle_{\mathrm{CFCMC}}} = P_{\mathrm{GE},j} \tag{6}$$

The difficulty associated with computing $P^*_{\mathrm{GE},j}$ using Eq. 6 is that only the states in which the value of λ equals zero are contributing to the ensemble average. Therefore, long simulations may be required to obtain reliable pressures especially for the liquid phase. Assuming that there is no correlation between the volume and the number of whole molecules, and also no

correlation between the volume and the virial part of the pressure, Eq. 6 reduces to

$$P^{**}_{\mathrm{GE},j} = k_B T \left\langle \frac{N_j}{V_j} \right\rangle_{\mathrm{CFCMC}} + \left\langle \frac{\sum_{a<b,a,\neg\mathrm{frac}} f_j(r_{ab,j}) r_{ab,j}}{3V_j} \right\rangle_{\mathrm{CFCMC}} \tag{7}$$

where the notation "¬frac" indicates that contribution of fractional molecule in virial part of the pressure should be disregarded. It is important to note that P^{**}_{GE} is an approximation for the pressure corresponding to the GE, and unlike P^{*}_{GE}, P_{GE}, and P_{CFCMC}, the quantity P^{**}_{GE} may not be equal for both simulation boxes. In the gas phase, particles are usually far enough from each other that the contribution of the virial part in the total pressure is limited and not correlated with the volume of the box. However, in the liquid phase, stronger correlation between the contribution of the viral part of the pressure and the volume of the box is expected. The validity of the simplification of Eq. 7 is numerically investigated in the next section. One can use the exact same approach to define different densities:

$$\rho_{\mathrm{GE},j} = \left\langle \frac{N_j}{V_j} \right\rangle_{\mathrm{GE}} \tag{8}$$

$$\rho_{\mathrm{CFCMC},j} = \left\langle \frac{N_j + \delta_{i,j}}{V_j} \right\rangle_{\mathrm{CFCMC}} \tag{9}$$

$$\rho^{*}_{\mathrm{GE},j} = \frac{\left\langle \delta_{\lambda=0,i=j} \frac{N_j}{V_j^2} \right\rangle_{\mathrm{CFCMC}}}{\left\langle \delta_{\lambda=0,i=j} \frac{1}{V_j} \right\rangle_{\mathrm{CFCMC}}} \tag{10}$$

$$\rho^{**}_{\mathrm{GE},j} = \left\langle \frac{N_j}{V_j} \right\rangle_{\mathrm{CFCMC}} \tag{11}$$

where $\rho_{\mathrm{GE},j}$ is the average density of box j computed in the conventional GE, $\rho_{\mathrm{CFCMC},j}$ is the average density of box j computed in the CFCMC GE (including the fractional molecule), $\rho^{*}_{\mathrm{GE},j}$ is the average density of box j computed in the CFCMC GE only when the value of λ equals zero excluding contribution of the fractional molecule, and $\rho^{**}_{\mathrm{GE},j}$ is the average density of box j computed in the CFCMC GE excluding the fractional molecule and averaged over all values of λ.

Simulation Details

To examine the validity of the equations provided in the Supporting Information, the VLE of a system with 256 and 512 LJ particles is investigated at three different reduced temperatures (T =0.7, 0.8, 0.95). The LJ potentials are truncated and shifted at $\sigma = 2.5$. Simulations are carried out in the conventional GE and the CFCMC GE. The LJ parameters σ and ϵ are used as units of length and energy respectively. Consequently, all calculated properties are in reduced units. A biasing function $W(\lambda, i)$ is computed iteratively to obtain a flat probability distribution of λ and that the fractional molecule is located with equal probability in both boxes. After 2 million equilibration cycles, a long production (500 million cycles) run is carried out to reduce the uncertainties in the values computed for pressures introduced in Eqs. 4 to 7. The number of Monte Carlo steps per cycle equals the total number of molecules in the system, with a minimum of 20. For more simulation details the reader is referred to Ref.[31]

Results

To compute the pressures and densities, simulations are performed in the conventional GE and the CFCMC GE. In Tables 1 and 2, the average pressures derived in Eqs. 4 to 7 and corresponding densities for the gas and liquid phases are shown for three different reduced temperatures (T =0.7, 0.8, 0.95) and for two system sizes (256 and 512 particles).

An important point in Tables 1 and 2 is the fact that the thermodynamic pressures of the two phases computed in the conventional GE (P_{GE}) are equal. The thermodynamic pressures of the two phases computed in CFCMC GE (P_{CFCMC}) are also equal. However, the thermodynamic pressures of the two ensembles, CFCMC GE and the conventional GE (P_{CFCMC}, and P_{GE}) are clearly not equal. As discussed in the previous section, the presence of the fractional molecule in the CFCMC GE simulations results in an increase in the thermodynamic pressure. However, the computed values for P^{*}_{GE} and P_{GE} are nearly identical. In the same

way, densities computed in CFCMC GE including the fractional molecule (ρ_{CFCMC}) are not equal to those computed in the conventional GE (ρ_{GE}). However, densities corresponding to the conventional GE but computed in CFCMC GE (ρ^{*}_{GE}) are equal to densities computed in the conventional GE (ρ_{GE}). This numerically confirms the validity of the derivations provided for computing properties corresponding to the conventional GE in the CFCMC GE. Only the states in which the value of λ is zero are contributing to the P^{*}_{GE}. As a result, the uncertainties associated with P^{*}_{GE} values are much larger than the other ensemble averages.

The values of P^{**}_{GE} computed for the gas phase are very close to the values computed for P_{GE} and P^{*}_{GE} (deviation less than 0.2%). This is not the case for P^{**}_{GE} computed for the liquid phase (deviation up to 4%). The gas phase density of the conventional GE can be accurately estimated using ρ^{**}_{GE} (see Tables 1 and 2). Since the contribution of the virial part in the pressure of the gas phase is negligible and the ideal gas part is defined by the density, P^{**}_{GE} for the gas phase can be used as an estimate of P^{*}_{GE} and P_{GE}.

In the liquid phase, the presence of a fractional molecule (with scaling parameter larger than zero) may influence the density and structure of the liquid phase. Radial Distribution Functions (RDFs) can be used to investigate the effect of the fractional molecule on the structure of the phases. The CFCMC GE system can be considered as a binary system, therefore, there are three different RDFs $g_{\mathrm{WW}}(r)$ (Whole-Whole), $g_{\mathrm{WF}}(r)$ (Whole-Fractional), and $g_{FF}(r)$ (Fractional-Fractional). Since there is only one fractional molecule, $g_{FF}(r)$ is always zero. In Fig. 2, $g_{\mathrm{WW}}(r)$ and $g_{\mathrm{WF}}(r)$ are plotted for different densities and values of λ. To reduce the number of particles and amplify the effect of the fractional molecule, the cutoff radius is reduced to 2σ and minimum box size and number of particles are used for these simulations. Simulations are performed in the NVT ensemble with only a single fractional molecule with a fixed value of λ. As shown in Fig. 2, $g_{\mathrm{WW}}(r)$ are almost identical for all values of λ. To test the extreme case, the interactions of the fractional molecule with the whole molecules were changed in such a way that the fractional molecule is acting as an attraction site without any repulsive potential ($u_{\mathrm{LJ}} = -a\lambda\sigma^{6}/(\sigma^{6} + r^{6})$). For $\lambda = 1$ and

$a < 60k_BT$, hardly any changes were observed in the RDFs, when the density was close to typical liquid densities (not shown here). This indicates that the structure of the liquid is not affected by the fractional molecule.

In Fig. 3a, the dependency of the density (excluding the fractional molecule) to the value of λ is investigated. An interesting point is that the densities corresponding to the conventional GE are only recovered when the value of λ is close to zero. It can be observed that the density of the gas phase increases and the density of the liquid phase decreases as λ changes from 0 to 1. In Fig. 3b, the unbiased probability distribution of λ in the two phases is shown. The fractional molecule is most of the times in the liquid phase. As a result, ρ^{**}_{GE} for the gas phase is close to ρ^{*}_{GE} for the gas phase. It can be seen that the fractional molecule is most of the times in the liquid phase with λ close to one. In this case, the density of the liquid phase in underestimated. Therefore, one would expect the ρ^{**}_{GE} to be slightly lower than the values of ρ^{*}_{GE} for the liquid phase. This is confirmed by data presented in Tables 1 and 2. Underestimation of the density of the liquid phase can influence both the ideal part and virial contribution of ρ^{**}_{GE}. This explains why the values reported for P^{**}_{GE} are slightly off.

Conclusions

In this study, we showed that there are differences between the averages computed in the CFCMC GE and those computed in the conventional GE. Although these differences may be limited for many properties, it is important to know that they exist. For example, the thermodynamic pressures in the conventional GE and CFCMC GE are different and typically differ by at most 3% for a system of 256 LJ particles. We also introduced guidelines for computing the averages corresponding to the conventional GE and computed in the CFCMC GE. We showed analytically and numerically that these values are identical to values computed in the conventional GE. As an example, we computed the pressure and density in

the conventional GE and CFCMC GE introduced by Poursaeidesfahani et al.[31] The pressure and densities corresponding to the conventional GE and computed in the CFCMC GE are equal to the pressure and densities computed in the conventional GE. However, due to the limited sampling (only when $\lambda = 0$) of these averages in CFCMC GE, long simulations are required to obtain reliable results. For the gas phase, the pressure is predominately defined by the ideal gas part. Therefore, using the estimation provided by Eq. 7 (i.e. ignoring the fractional molecule in the ideal gas part and the virial part), one can compute the pressure corresponding to the conventional GE from the gas phase of a CFCMC GE simulation and still sampling for all values of λ. We also showed that the structures of the two phases are not influenced by the fractional molecule.

Acknowledgments

This work was sponsored by NWO Exacte Wetenschappen (Physical Sciences) for the use of supercomputer facilities, with financial support from the Nederlandse Organisatie voor Wetenschappelijk Onderzoek (Netherlands Organization for Scientific Research, NWO). The authors also gratefully acknowledge the financial support from Shell Global Solutions B.V., and the Netherlands Research Council for Chemical Sciences (NWO/CW) through a VIDI grant (David Dubbeldam) and a VICI grant (Thijs J. H. Vlugt).

Table 1: Computed pressures and densities in the conventional GE and the CFCMC GE at different reduced temperatures for 256 LJ particles. $P_{\rm GE}$ (Eq. 4) and $P_{\rm CFCMC}$ (Eq. 5) are the pressures in the conventional GE and the CFCMC GE, respectively. $P^{*}_{\rm GE}$ (Eq. 6) indicates the pressure corresponding to that in the conventional GE and computed in the CFCMC GE. $P^{**}_{\rm GE}$ (Eq. 7) is the computed pressure in the CFCMC GE, not counting the contributions of the fractional molecule. The exact same definitions apply to the computed densities (Eqs. 8 to 11). Statistical uncertainties in the last digit are shown in brackets, i.e, 14.21(1) means 14.21 ± 0.01. The weight function in the CFCMC GE is calculated iteratively so that the probability distribution $p(\lambda, j)$ is uniform. The total volume for $T = 0.8$ and $T = 0.95$ is $V_T = 2 \times 8^3$ and for $T = 0.7$ is $V_T = 2 \times 12.5^3$.

	[Average Pressure]/10^{-3}			[Average Density]/10^{-3}	
$T = 0.7$	Gas	Liquid		Gas	Liquid
$P_{\rm CFCMC}$	4.89(1)	4.90(10)	$\rho_{\rm CFCMC}$	7.42(1)	786.44(9)
$P_{\rm GE}$	4.78(1)	4.75(5)	$\rho_{\rm GE}$	7.25(1)	786.50(0)
$P^{*}_{\rm GE}$	4.78(1)	4.70(60)	$\rho^{*}_{\rm GE}$	7.26(1)	786.50(0)
$P^{**}_{\rm GE}$	4.77(1)	5.10(50)	$\rho^{**}_{\rm GE}$	7.26(1)	785.00(0)
$T = 0.8$	Gas	Liquid		Gas	Liquid
$P_{\rm CFCMC}$	14.21(1)	14.20(10)	$\rho_{\rm CFCMC}$	20.31(2)	731.00(0)
$P_{\rm GE}$	13.86(0)	13.87(6)	$\rho_{\rm GE}$	19.84(0)	731.16(9)
$P^{*}_{\rm GE}$	13.87(1)	13.80(50)	$\rho^{*}_{\rm GE}$	19.83(3)	731.16(9)
$P^{**}_{\rm GE}$	13.87(1)	14.20(10)	$\rho^{**}_{\rm GE}$	19.84(2)	729.00(0)
$T = 0.95$	Gas	Liquid		Gas	Liquid
$P_{\rm CFCMC}$	45.02(3)	45.02(4)	$\rho_{\rm CFCMC}$	66.80(10)	623.02(8)
$P_{\rm GE}$	44.44(3)	44.42(6)	$\rho_{\rm GE}$	66.02(7)	623.30(10)
$P^{*}_{\rm GE}$	44.42(6)	44.40(50)	$\rho^{*}_{\rm GE}$	65.90(20)	623.30(0)
$P^{**}_{\rm GE}$	44.50(7)	44.81(3)	$\rho^{**}_{\rm GE}$	66.10(10)	621.52(8)

Table 2: Computed pressures and densities in the conventional GE and the CFCMC GE at different reduced temperatures for 512 LJ particles. $P_{\rm GE}$ (Eq. 4) and $P_{\rm CFCMC}$ (Eq. 5) are the pressures in the conventional GE and the CFCMC GE, respectively. $P^{*}_{\rm GE}$ (Eq. 6) indicates the pressure corresponding to that in the conventional GE and computed in the CFCMC GE. $P^{**}_{\rm GE}$ (Eq. 7) is the computed pressure in the CFCMC GE, not counting the contributions of the fractional molecule. The exact same definitions apply to the computed densities (Eqs. 8 to 11). Statistical uncertainties in the last digit are shown in brackets, i.e, 14.10(1) means 14.10 ± 0.01. The weight function in the CFCMC GE is calculated iteratively so that the probability distribution $p(\lambda, j)$ is uniform. The total volume for $T = 0.7$ is $V_T = 2 \times 14.5^3$ and for $T = 0.8$, $V_T = 2 \times 10^3$ and for $T = 0.95$, the total volume is $V_T = 2 \times 8.65^3$.

	[Average Pressure]/10^{-3}			[Average Density]/10^{-3}	
$T = 0.7$	Gas	Liquid		Gas	Liquid
$P_{\rm CFCMC}$	4.95(1)	4.95(6)	$\rho_{\rm CFCMC}$	7.53(2)	787.0(0)
$P_{\rm GE}$	4.89(0)	4.89(4)	$\rho_{\rm GE}$	7.44(1)	787.09(1)
$P^{*}_{\rm GE}$	4.89(1)	4.80(50)	$\rho^{*}_{\rm GE}$	7.44(2)	787.02(4)
$P^{**}_{\rm GE}$	4.88(1)	5.01(3)	$\rho^{**}_{\rm GE}$	7.44(2)	786.20(0)
$T = 0.8$	Gas	Liquid		Gas	Liquid
$P_{\rm CFCMC}$	14.10(1)	14.14(3)	$\rho_{\rm CFCMC}$	20.17(2)	730.84(7)
$P_{\rm GE}$	13.92(1)	13.91(2)	$\rho_{\rm GE}$	19.92(1)	730.95(4)
$P^{*}_{\rm GE}$	13.93(1)	13.90(20)	$\rho^{*}_{\rm GE}$	19.92(1)	730.93(4)
$P^{**}_{\rm GE}$	13.92(1)	14.10(10)	$\rho^{**}_{\rm GE}$	19.92(2)	729.83(4)
$T = 0.95$	Gas	Liquid		Gas	Liquid
$P_{\rm CFCMC}$	44.88(3)	44.86(5)	$\rho_{\rm CFCMC}$	66.67(7)	623.39(4)
$P_{\rm GE}$	44.51(2)	44.51(2)	$\rho_{\rm GE}$	65.00(90)	623.60(10)
$P^{*}_{\rm GE}$	44.50(1)	44.60(10)	$\rho^{*}_{\rm GE}$	66.10(10)	623.60(10)
$P^{**}_{\rm GE}$	44.53(2)	44.76(8)	$\rho^{**}_{\rm GE}$	66.20(7)	622.30(10)

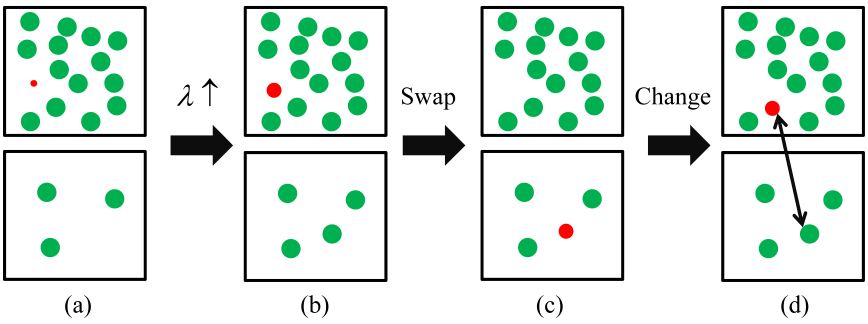

Figure 1: Schematic representation of the additional trial moves in CFCMC GE. The red sphere is the fractional molecule and the green spheres are the whole molecules. (a)→(b): changing the scaling parameter λ with $\lambda \in [0, 1]$. (b)→(c): swapping the fractional molecule between the boxes. (c)→(d): changing the identity of the fractional molecule with a randomly selected whole molecule in the other simulation box, while keeping the value of λ constant.

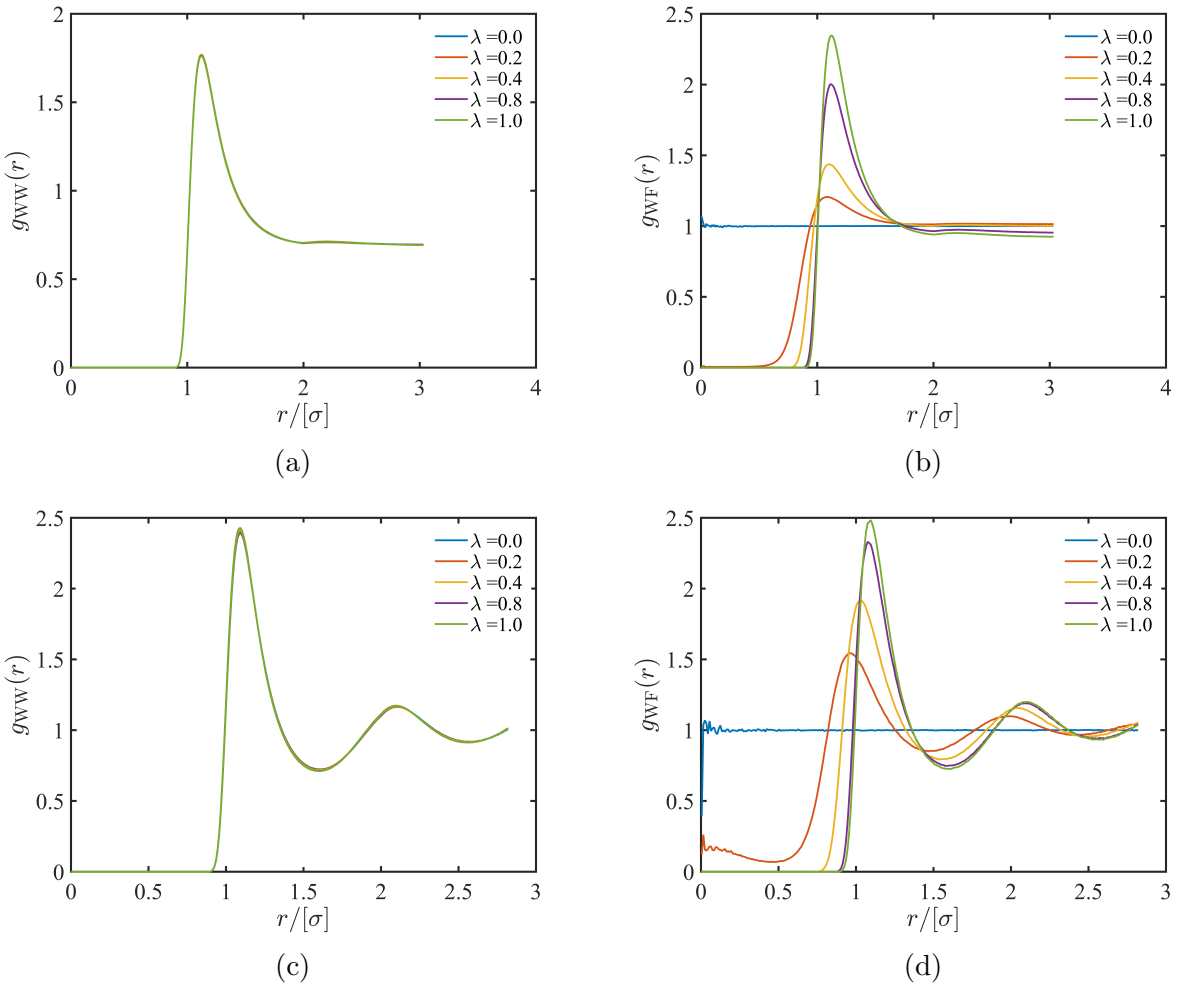

Figure 2: (a) Radial distribution functions $g_{\mathrm{WW}}(r)$ and (b) $g_{\mathrm{WF}}(r)$ for 4 LJ particles at $T = 1$ and $\rho = 0.05$. (c) Radial distribution functions $g_{\mathrm{WW}}(r)$ and (d) $g_{\mathrm{WF}}(r)$ for 40 LJ particles at $T = 1$ and $\rho = 0.8$. To reduce the number of particles and amplify the effect of the fractional molecule, the cutoff radius is reduced to 2σ.

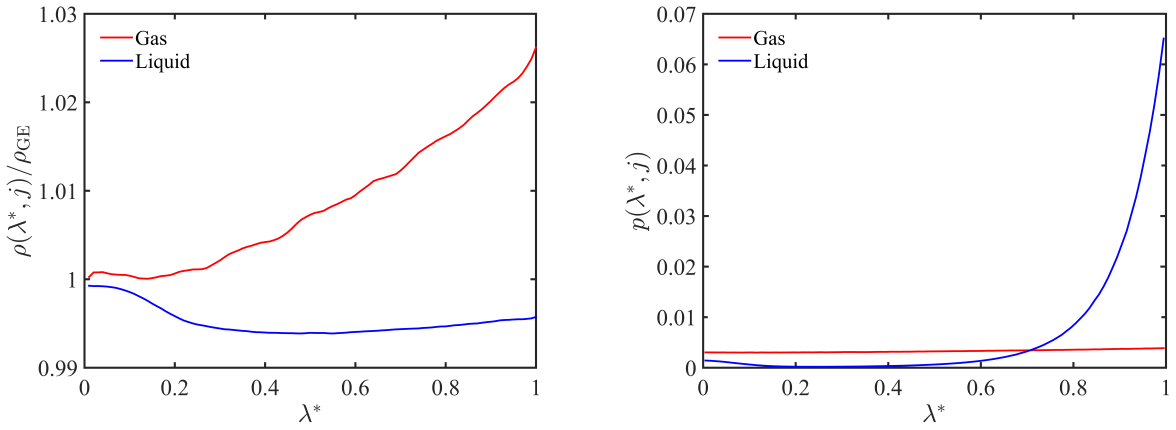

Figure 3: (a) $\rho(\lambda^*, j)/\rho_{\mathrm{GE}}$ for the two phases as a function λ. $\rho(\lambda^*, j) = \frac{\left\langle \delta_{\lambda=\lambda^*, i=j} \frac{N_j}{V_j} \right\rangle_{\mathrm{CFCMC}}}{\left\langle \delta_{\lambda=\lambda^*, i=j} \right\rangle_{\mathrm{CFCMC}}}$ is the density of box j averaged over the configurations in which the fractional particle is in box j with $\lambda = \lambda^*$. Note: in calculation of these densities, the fractional molecule was disregarded. (b) Probability distribution of λ for the two phases for 256 LJ particles at $T = 0.8$.

References

1. Walas, S. M. *Phase equilibria in chemical engineering*; Butterworth, Boston, 1985.

2. Nebig, S.; Gmehling, J. Prediction of phase equilibria and excess properties for systems with ionic liquids using modified UNIFAC: Typical results and present status of the modified UNIFAC matrix for ionic liquids. *Fluid Phase Equilib.* **2011**, *302*, 220–225.

3. Neroorkar, K.; Schmidt, D. Modeling of vapor-liquid equilibrium of gasoline-ethanol blended fuels for flash boiling simulations. *Fuel* **2011**, *90*, 665–673.

4. Potoff, J. J.; Siepmann, J. I. Vapor-liquid equilibria of mixtures containing alkanes, carbon dioxide, and nitrogen. *AlChE J.* **2001**, *47*, 1676–1682.

5. Errington, J. R.; Boulougouris, G. C.; Economou, I. G.; Panagiotopoulos, A. Z.; Theodorou, D. N. Molecular simulation of phase equilibria for water-methane and water-ethane mixtures. *J. Phys. Chem. B* **1998**, *102*, 8865–8873.

6. Vorholz, J.; Harismiadis, V.; Rumpf, B.; Panagiotopoulos, A. Z.; Maurer, G. Vapor-liquid equilibrium of water, carbon dioxide, and the binary system, water+carbon dioxide, from molecular simulation. *Fluid Phase Equilib.* **2000**, *170*, 203–234.

7. Panagiotopoulos, A. Z. Direct determination of phase coexistence properties of fluids by Monte Carlo simulation in a new ensemble. *Mol. Phys.* **1987**, *61*, 813–826.

8. Baus, M.; Rull, L. F.; Ryckaert, J.-P. *Observation, prediction and simulation of phase transitions in complex fluids*; Edinburgh, Springer Science & Business Media, 2012; Vol. 460.

9. Panagiotopoulos, A. Z.; Quirke, N.; Stapleton, M.; Tildesley, D. Phase equilibria by simulation in the Gibbs ensemble: alternative derivation, generalization and application to mixture and membrane equilibria. *Mol. Phys.* **1988**, *63*, 527–545.

10. Neubauer, B.; Boutin, A.; Tavitian, B.; Fuchs, A. H. Gibbs ensemble simulations of vapour-liquid phase equilibria of cyclic alkanes. *Mol. Phys.* **1999**, *97*, 769–776.

11. De Pablo, J. J.; Prausnitz, J. M. Phase equilibria for fluid mixtures from Monte-Carlo simulation. *Fluid Phase Equilib.* **1989**, *53*, 177–189.

12. Green, D. G.; Jackson, G.; de Miguel, E.; Rull, L. F. Vapor-liquid and liquid-liquid phase equilibria of mixtures containing square-well molecules by Gibbs ensemble Monte Carlo simulation. *J. Chem. Phys.* **1994**, *101*, 3190–3204.

13. Fetisov, E. O.; Siepmann, J. I. Prediction of vapor-Liquid coexistence properties and critical points of polychlorinated biphenyls from Monte Carlo simulations with the TraPPE force field. *J. Chem. Eng. Data* **2015**, *60*, 3039–3045.

14. Dinpajooh, M.; Bai, P.; Allan, D. A.; Siepmann, J. I. Accurate and precise determination of critical properties from Gibbs ensemble Monte Carlo simulations. *J. Chem. Phys.* **2015**, *143*, 114113.

15. Ferrenberg, A. M.; Swendsen, R. H. Optimized Monte Carlo data analysis. *Phys. Rev. Lett.* **1989**, *63*, 1195–1198.

16. Ferrenberg, A. M.; Swendsen, R. H. New Monte Carlo technique for studying phase transitions. *Phys. Rev. Lett.* **1988**, *61*, 2635–2638.

17. Poursaeidesfahani, A.; Torres-Knoop, A.; Rigutto, M.; Nair, N.; Dubbeldam, D.; Vlugt, T. J. H. Computation of the heat and entropy of adsorption in proximity of inflection points. *J. Phys. Chem. C* **2016**, *120*, 1727–1738.

18. Rane, K. S.; Murali, S.; Errington, J. R. Monte Carlo simulation methods for computing liquid-vapor saturation properties of model systems. *J. Chem. Theory Comput.* **2013**, *9*, 2552–2566.

19. Escobedo, F. A.; de Pablo, J. J. Monte Carlo simulation of the chemical potential of polymers in an expanded ensemble. *J. Chem. Phys.* **1995**, *103*, 2703–2710.

20. Lyubartsev, A. P.; Martsinovski, A. A.; Shevkunov, S. V.; Vorontsov-Velyaminov, P. N. New approach to Monte Carlo calculation of the free energy: Method of expanded ensembles. *J. Chem. Phys.* **1992**, *96*, 1776–1783.

21. Shi, W.; Maginn, E. J. Continuous Fractional Component Monte Carlo: An adaptive biasing method for open system atomistic simulations. *J. Chem. Theory Comput.* **2007**, *3*, 1451–1463.

22. Shi, W.; Maginn, E. J. Improvement in molecule exchange efficiency in Gibbs ensemble Monte Carlo: Development and implementation of the continuous fractional component move. *J. Comput. Chem.* **2008**, *29*, 2520–2530.

23. Shi, W.; Maginn, E. J. Atomistic simulation of the absorption of carbon dioxide and water in the ionic liquid 1-n-Hexyl-3-methylimidazolium bis(trifluoromethylsulfonyl)imide ([hmim][Tf2N]. *J. Phys. Chem. B* **2008**, *112*, 2045–2055.

24. Maginn, E. J. Atomistic simulation of the thermodynamic and transport properties of ionic liquids. *Acc. Chem. Res.* **2007**, *40*, 1200–1207.

25. Kelkar, M. S.; Shi, W.; Maginn, E. J. Determining the accuracy of classical force fields for ionic liquids: atomistic simulation of the thermodynamic and transport properties of 1-Ethyl-3-methylimidazolium ethylsulfate ([emim][EtSO4]) and its mixtures with water. *Ind. Eng. Chem. Res.* **2008**, *47*, 9115–9126.

26. Zhang, X.; Huo, F.; Liu, Z.; Wang, W.; Shi, W.; Maginn, E. J. Absorption of CO_2 in the ionic liquid 1-n-hexyl-3-methylimidazolium tris(pentafluoroethyl)trifluorophosphate ([hmim][FEP]): A molecular view by computer simulations. *J. Phys. Chem. B* **2009**, *113*, 7591–7598.

27. Chen, Q.; Balaji, S. P.; Ramdin, M.; Gutiarrez-Sevillano, J. J.; Bardow, A.; Goetheer, E.; Vlugt, T. J. H. Validation of the CO_2/N_2O analogy using molecular simulation. *Ind. Eng. Chem. Res.* **2014**, *53*, 18081–18090.

28. Ramdin, M.; Balaji, S. P.; Vicent-Luna, J. M.; Gutirrez-Sevillano, J. J.; Calero, S.; de Loos, T. W.; Vlugt, T. J. H. Solubility of the precombustion gases CO_2, CH_4, CO, H_2, N_2, and H_2S in the ionic liquid [bmim][Tf2N] from Monte Carlo simulations. *J. Phys. Chem. C* **2014**, *118*, 23599–23604.

29. Ramdin, M.; Balaji, S. P.; Torres-Knoop, A.; Dubbeldam, D.; de Loos, T. W.; Vlugt, T. J. H. Solubility of Natural Gas Species in Ionic Liquids and Commercial Solvents: Experiments and Monte Carlo Simulations. *J. Chem. Eng. Data* **2015**, *60*, 3039–3045.

30. Shi, W.; Siefert, N. S.; Morreale, B. D. Molecular Simulations of CO_2, H_2, H_2O, and H_2S gas absorption into hydrophobic poly(dimethylsiloxane) (PDMS) solvent: Solubility and surface tension. *J. Phys. Chem. C* **2015**, *119*, 19253–19265.

31. Poursaeidesfahani, A.; Torres-Knoop, A.; Dubbeldam, D.; Vlugt, T. J. H. Direct free energy calculation in the continuous fractional component Gibbs ensemble. *J. Chem. Theo. Comp.* **2016**, *12*, 1481–1490.

32. Poursaeidesfahani, A.; Torres-Knoop, A.; Dubbeldam, D.; Vlugt, T. J. H. doi:10.4121/uuid:14e501bc-2408-41bc-90d5-5f4588604849.

33. de Miguel, E.; Jackson, G. The nature of the calculation of the pressure in molecular simulations of continuous models from volume perturbations. *J. Chem. Phys.* **2006**, *125*, 164109.

34. Gray, C. G.; Gubbins, K. E.; Joslin, C. G. *Theory of molecular fluids 2: Applications. international series of monographs on chemistry*; Oxford University Press, New York, 2011.

35. Allen, M. P.; Tildesley, D. J. *Computer simulation of liquids*; Oxford University Press: New York, 1989.

36. Frenkel, D.; Smit, B. *Understanding molecular simulation: from algorithms to applications*; Academic Press: San Diego, California, 2002.

Supporting Information for: Computation of Thermodynamic Properties in the Continuous Fractional Component Monte Carlo Gibbs Ensemble

Ali Poursaeidesfahani,[†] Ahmadreza Rahbari,[†] Ariana Torres-Knoop,[‡] David Dubbeldam,[‡] and Thijs J.H. Vlugt[*,†]

Engineering Thermodynamics, Process & Energy Department, Faculty of Mechanical, Maritime and Materials Engineering, Delft University of Technology, Leeghwaterstraat 39, 2628CB, Delft, The Netherlands, and Van't Hoff Institute for Molecular Sciences, University of Amsterdam, Science Park 904, 1098XH Amsterdam, The Netherlands

E-mail: t.j.h.vlugt@tudelft.nl

[*]To whom correspondence should be addressed
[†]Delft University of Technology
[‡]Van't Hoff Institute for Molecular Sciences

In this Supporting Information, expressions are derived to compute the pressure in the conventional Gibbs Ensemble (GE), the Continuous Fractional Component Monte Carlo Gibbs Ensemble (CFCMC GE), and the pressure corresponding to the conventional GE which is computed in the CFCMC GE. The latter derivation can be easily modified to compute any thermodynamic property corresponding to the conventional GE but computed in the CFCMC GE. This will be shown explicitly at the end of this document. In these derivations, pair potentials are assumed, but the resulting expressions can be easily generalized to other types of interactions.

Pressure the in Conventional GE

Starting from the conventional GE one can write for the partition function:[1,2]

$$Q_{\mathrm{GE}} = \frac{1}{\Lambda^{3(N_T)}\,(N_T)!} \sum_{N_1=0}^{N_T} \binom{N_T}{N_1} \int_0^{V_T} dV_1 {V_1}^{N_1} (V_T - V_1)^{N_T - N_1} \int ds^{N_1} \exp[-\beta U_1(s^{N_1}, V_1)] \times \int ds^{N_T - N_1} \exp[-\beta U_2(s^{N_T - N_1}, (V_T - V_1))] \tag{S1}$$

The total number of particles and the total volume are constant

$$\begin{aligned} N_T &= N_1 + N_2 \\ V_T &= V_1 + V_2 \end{aligned} \tag{S2}$$

Λ is the thermal wavelength. The subscripts 1 and 2 indicate the simulation box. N_T is the total number of particles, and V_T denotes the total volume of the two boxes. The reduced coordinates are denoted with s, and U_j is the total energy of box j. The thermodynamic

pressure in the conventional GE is derived from the partition function:

$$P_{\mathrm{GE}} = k_B T \left(\frac{\partial \ln Q_{\mathrm{GE}}}{\partial V_T} \right)_T \tag{S3}$$

This leads to

$$\frac{\partial \ln Q_{\mathrm{GE}}}{\partial V_T} = \frac{1}{\Lambda^{3(N_T)}\,(N_T)!} \frac{1}{Q_{\mathrm{GE}}} \sum_{N_1=0}^{N_T} \binom{N_T}{N_1} \frac{\partial}{\partial V_T} \left[\begin{array}{l} \int_0^{V_T} dV_1 {V_1}^{N_1} (V_T - V_1)^{N_T - N_1} \int ds^{N_1} \exp[-\beta U_1(s^{N_1}, V_1)] \\ \times \int ds^{N_T - N_1} \exp[-\beta U_2(s^{N_T - N_1}, (V_T - V_1))] \end{array} \right] \tag{S4}$$

V_1 is the running variable over which we integrate. It is important to note that the labeling of the boxes is arbitrary, and therefore we will obtain a similar expression if we would integrate over V_2. We will see that integrating over V_1 yields and expression for the pressure in box 2, and vice versa. Therefore, by definition, the average pressures of both boxes are exactly identical.

The total volume V_T is present inside the integral and also in the limits of the integral. Therefore, the theorem for differentiation under the integral sign and product rule applies here.[3] This leads to

$$\frac{\partial \ln Q_{\mathrm{GE}}}{\partial V_T} = \frac{1}{\Lambda^{3(N_T)}\,(N_T)!} \frac{1}{Q_{\mathrm{GE}}} \sum_{N_1=0}^{N_T} \binom{N_T}{N_1} \int_0^{V_T} dV_1 \frac{\partial}{\partial V_T} \left[\begin{array}{l} {V_1}^{N_1} (V_T - V_1)^{N_T - N_1} \int ds^{N_1} \exp[-\beta U_1(s^{N_1}, V_1)] \\ \int ds^{N_T - N_1} \exp[-\beta U_2(s^{N_T - N_1}, (V_T - V_1))] \end{array} \right] \tag{S5}$$

By applying the product rule to the terms inside the brackets, we obtain:

$$\begin{aligned} \frac{\partial \ln Q_{\mathrm{GE}}}{\partial V_T} = & \frac{1}{\Lambda^{3(N_T)}\,(N_T)!} \frac{1}{Q_{\mathrm{GE}}} \sum_{N_1=0}^{N_T} \binom{N_T}{N_1} \int_0^{V_T} dV_1 \left[\begin{array}{l} {V_1}^{N_1} (N_T - N_1) (V_T - V_1)^{N_T - N_1 - 1} \int ds^{N_1} \exp[-\beta U_1(s^{N_1}, V_1)] \\ \int ds^{N_T - N_1} \exp[-\beta U_2(s^{N_T - N_1}, (V_T - V_1))] \end{array} \right] \\ & + \frac{1}{\Lambda^{3(N_T)}\,(N_T)!} \frac{1}{Q_{\mathrm{GE}}} \sum_{N_1=0}^{N_T} \binom{N_T}{N_1} \int_0^{V_T} dV_1 \left[\begin{array}{l} {V_1}^{N_1} (V_T - V_1)^{N_T - N_1} \frac{\partial}{\partial V_T} \int ds^{N_1} \exp[-\beta U_1(s^{N_1}, V_1)] \\ \int ds^{N_T - N_1} \exp[-\beta U_2(s^{N_T - N_1}, (V_T - V_1))] \end{array} \right] \end{aligned} \tag{S6}$$

In the first term of the right hand side of Eq. S6, we rewrite ${V_1}^{N_1}(N_T - N_1)(V_T - V_1)^{N_T - N_1 - 1}$ as ${V_1}^{N_1}(\frac{N_2}{V_2}){V_2}^{N_2}$. Note that $\frac{N_2}{V_2}$ equals the density in box 2. Therefore

$$\frac{\partial \ln Q_{\mathrm{GE}}}{\partial V_T} = \frac{1}{\Lambda^{3(N_T)}\,(N_T)!}\frac{1}{Q_{\mathrm{GE}}}\sum_{N_1=0}^{N_T}\binom{N_T}{N_1}\int_0^{V_T} dV_1 \begin{bmatrix} {V_1}^{N_1}(\frac{N_2}{V_2}){V_2}^{N_2}\int ds^{N_1}\exp[-\beta U_1(s^{N_1}, V_1)] \\ \int ds^{N_T-N_1}\exp[-\beta U_2(s^{N_T-N_1}, V_2)] \end{bmatrix}$$
$$+ \frac{1}{\Lambda^{3(N_T)}\,(N_T)!}\frac{1}{Q_{\mathrm{GE}}}\sum_{N_1=0}^{N_T}\binom{N_T}{N_1}\int_0^{V_T} dV_1 \begin{bmatrix} {V_1}^{N_1}(V_T - V_1)^{N_T-N_1}\frac{\partial}{\partial V_T}\int ds^{N_1}\exp[-\beta U_1(s^{N_1}, V_1)] \\ \int ds^{N_T-N_1}\exp[-\beta U_2(s^{N_T-N_1}, (V_T - V_1))] \end{bmatrix} \quad \text{(S7)}$$

Now we will mathematically manipulate the second term in Eq. S7 to obtain the well-known virial part.[4] We can write $V_2 = V_T - V_1$ and as a result $dV_2 = dV_T - dV_1$. Since V_1 is the running variable of the integrals in Eq. S7 and V_T is constant, we obtain: $dV_2 = dV_T$. In the second term of the right hand side of Eq. S7, we take the derivative with respect to V_T (or V_2) inside the integral over box 2. Then this integral becomes

$$\int ds^{N_T-N_1}\frac{\partial}{\partial V_2}\exp\left[-\beta U_2\left(s^{N_2}, V_2\right)\right] = \int ds^{N_T-N_1}\sum_{a<b}\frac{\partial\left(-\beta u_2\left(s_{ab}, V_2\right)\right)}{\partial V_2}\exp\left[-\beta U_2\left(s^{N_2}, V_2\right)\right] \quad \text{(S8)}$$

To obtain the virial part, we loop over all pair particles (denoted by a and b in the summation) in the simulation box. s_{ab} denotes the reduced distance between a and b, and $u_2\left(s_{ab}, V_2\right)$ is the pair potential calculated between the pair particles. Next, we change the derivative with respect to the volume to the derivative with respect to actual coordinates between particle pairs a and b. Starting from $V_2 = L_2^3$, we derive the partial derivative of the pair potential as a function of real coordinates. For box 2, we have

$$dV_2 = 3L_2^2 dL_2 \quad \text{(S9)}$$

Taking the derivative of the pair potential with respect to volume, we obtain for box 2

$$\frac{\partial}{\partial V_2}\sum_{a<b}u\left(r_{ab}\right)=\sum_{a<b}\frac{\partial u_{ab,2}}{\partial r_{ab,2}}\frac{dr_{ab,2}}{dV_2}=\frac{1}{3V_2}\sum_{a<b}\frac{\partial u\left(r_{ab,2}\right)}{\partial r_{ab,2}}r_{ab,2} \tag{S10}$$

With the virial part derived, we use Eq. S10 to rewrite Eq. S7

$$\frac{\partial \ln Q_{\mathrm{GE}}}{\partial V_T}=\frac{1}{\Lambda^{3(N_T)}\left(N_T\right)!}\frac{1}{Q_{\mathrm{GE}}}\sum_{N_1=0}^{N_T}\binom{N_T}{N_1}\int_0^{V_T}dV_1\left[\begin{array}{l}{V_1}^{N_1}\dfrac{N_2}{V_2}{V_2}^{N_2}\displaystyle\int ds^{N_1}\exp[-\beta U_1(s^{N_1},V_1)]\\ \displaystyle\int ds^{N_T-N_1}\exp[-\beta U_2(s^{N_2},V_2)]\end{array}\right]$$
$$+\frac{1}{\Lambda^{3(N_T)}\left(N_T\right)!}\frac{1}{Q_{\mathrm{GE}}}\sum_{N_1=0}^{N_T}\binom{N_T}{N_1}\int_0^{V_T}dV_1{V_1}^{N_1}{V_2}^{N_2}\times\left[\begin{array}{l}\displaystyle\int ds^{N_1}\exp[-\beta U_1(s^{N_1},V_1)]\frac{1}{3V_2}\times\\ \displaystyle\int ds^{N_T-N_1}\sum_{a<b}\frac{\partial\left(-\beta u_2\left(r_{ab},V_2\right)\right)}{\partial r_{ab,2}}r_{ab,2}\exp\left[-\beta U_2(s^{N_T-N_1},V_2)\right]\end{array}\right] \tag{S11}$$

The right hand side of Eq. S11, contains two ensemble averages. The first term represents the average denisty of box 2, and the second part becomes the average virial part. This leads to

$$\left\langle\frac{N_2}{V_2}\right\rangle_{\mathrm{GE}}=\frac{1}{\Lambda^{3(N_T)}\left(N_T\right)!}\frac{1}{Q_{\mathrm{GE}}}\sum_{N_1=0}^{N_T}\binom{N_T}{N_1}\int_0^{V_T}dV_1\left[\begin{array}{l}{V_1}^{N_1}\dfrac{N_2}{(V_2)}{V_2}^{N_2}\displaystyle\int ds^{N_1}\exp[-\beta U_1(s^{N_1},V_1)]\\ \displaystyle\int ds^{N_T-N_1}\exp[-\beta U_2(s^{N_2},V_2)]\end{array}\right] \tag{S12}$$

and

$$\left\langle\frac{\sum_{a<b}f(r_{ab,2})r_{ab,2}}{3V_2}\right\rangle_{\mathrm{GE}}=\frac{1}{\Lambda^{3(N_T)}\left(N_T\right)!}\frac{1}{Q_{\mathrm{GE}}}\sum_{N_1=0}^{N_T}\binom{N_T}{N_1}\int_0^{V_T}dV_1$$
$$\left[{V_1}^{N_1}(V_2)^{N_2}\left[\begin{array}{l}\displaystyle\int ds^{N_1}\exp[-\beta U_1(s^{N_1},V_1)]\frac{1}{3V_2}\\ \displaystyle\int ds^{N_T-N_1}\sum_{a<b}f(r_{ab,2})r_{ab,2}\exp[-\beta U_2(s^{N_2},V_2)]\end{array}\right]\right] \tag{S13}$$

Combining Eq. S3, Eq. S11, Eq. S12, Eq. S13, leads to

$$P_{\mathrm{GE}} = k_B T \left(\frac{\partial \ln Q_{\mathrm{GE}}}{\partial V_T} \right) = k_B T \left\langle \frac{N_2}{V_2} \right\rangle_{\mathrm{GE}} + \left\langle \frac{\sum_{a<b} f(r_{ab,2}) r_{ab,2}}{3V_2} \right\rangle_{\mathrm{GE}} \tag{S14}$$

in which we have used $\langle ... \rangle_{\mathrm{GE}}$ to denote ensemble averages in the conventional GE. This expression is the same as the conventional expression to compute the pressure in the NVT ensemble.[2] Alternatively, one could integrate over the volume of box 2 in Eq. S1, and this would lead to a similar expression as Eq. S14 but now with the label "2" replaced by "1". As the labeling of the boxes is arbitrary, it is clear that the average pressure of the boxes are exactly identical.

Pressure in the CFCMC GE

The partition function of the CFCMC GE is defined as[5]

$$\begin{aligned} Q_{\mathrm{CFCMC}} = \frac{1}{\Lambda^{3(N_T+1)}\,(N_T)!} \sum_{i=1}^{2} \sum_{N_1=0}^{N_T} \binom{N_T}{N_1} \int_0^1 d\lambda \int_0^{V_T} dV_1 {V_1}^{N_1+\delta_{i,1}} (V_T - V_1)^{N_T - N_1 + \delta_{i,2}} \\ \times \int ds^{N_1} \exp[-\beta U_{\mathrm{int},1}(s^{N_1})] \int ds^{N_T - N_1} \exp[-\beta U_{\mathrm{int},2}(s^{N_T-N_1})] \\ \times \left[\delta_{i,1} \int ds^1_{\mathrm{frac}} \exp[-\beta U_{\mathrm{frac},1}(s^1_{\mathrm{frac}}, s^{N_1}, \lambda)] + \delta_{i,2} \int ds^2_{\mathrm{frac}} \exp[-\beta U_{\mathrm{frac},2}(s^2_{\mathrm{frac}}, s^{N_T-N_1}, \lambda)] \right] \end{aligned} \tag{S15}$$

the terms i in $\delta_{i,j}$ denotes the box in which the fractional molecule is present. If the fractional molecule is in box 1, $\delta_{i,1} = 1$ and $\delta_{i,2} = 0$ and vise versa. s_{frac} and U_{frac} are the reduced coordinates and the potential energy of the fractional molecule, respectively. Note that in the CFCMC GE partition function, N_T denotes the number of whole particles, and N_1 and N_2 are the number of whole particles in box 1 and box 2. Other symbols have similar meaning as explained in the previous section. The thermodynamic pressure in the CFCMC GE is

defined as

$$P_{\mathrm{CFCMC}} = k_B T \left(\frac{\partial \ln Q_{\mathrm{CFCMC}}}{\partial V_T} \right)_T \tag{S16}$$

Differentiation with respect to V_T leads to

$$\begin{aligned} \frac{\partial \ln Q_{\mathrm{CFCMC}}}{\partial V_T} = & \frac{1}{\Lambda^{3(N_T+1)}\,(N_T)!} \frac{1}{Q_{\mathrm{CFCMC}}} \sum_{N_1=0}^{N_T} \binom{N_T}{N_1} \int_0^1 d\lambda \\ & \frac{\partial}{\partial V_T} \left[\begin{array}{l} \displaystyle\int_0^{V_T} dV_1 {V_1}^{N_1+\delta_{i,1}} (V_T - V_1)^{N_T - N_1 + \delta_{i,2}} \int ds^{N_1} \exp(-\beta U_{\mathrm{int},1}(s^{N_1}, V_1)) \\ \times \displaystyle\int ds^{N_T - N_1} \exp(-\beta U_{\mathrm{int},2}(s^{N_T-N_1}, (V_T - V_1))) \\ \times \left(\begin{array}{l} \delta_{i,1} \displaystyle\int ds^1_{\mathrm{frac}} \exp(-\beta U_{\mathrm{frac},1}(s_{\mathrm{frac}}, \lambda, V_1)) + \\ \delta_{i,2} \displaystyle\int ds^2_{\mathrm{frac}} \exp(-\beta U_{\mathrm{frac},2}(s_{\mathrm{frac}}, \lambda, (V_T - V_1))) \end{array} \right) \end{array} \right] \end{aligned} \tag{S17}$$

The term V_T is present both in the integrand and as one of the integral limits. Again we make use of theorem for differentiation under the integral and use the product rule.[3] It is important to note that the labeling of the boxes is arbitrary. This implies that we obtain the same mathematical expression for both boxes and, furthermore, it implies that the pressures computed in both boxes should be exactly identical. This leads to

$$\frac{\partial \ln Q_{\mathrm{CFCMC}}}{\partial V_1} = \frac{\frac{1}{Q_{\mathrm{CFCMC}}}}{\Lambda^{3(N_T+1)}\,(N_T)!} \sum_{N_1=0}^{N_T} \binom{N_T}{N_1} \int_0^1 d\lambda \int_0^{V_T} dV_1 \left[\begin{array}{l} {V_1}^{N_1+\delta_{i,1}}\,(N_T - N_1 + \delta_{i,2})\,(V_T - V_1)^{N_T-N_1+\delta_{i,2}-1} \\ \times \int ds^{N_1} \exp(-\beta U_{\mathrm{int},1}(s^{N_1}, V_1)) \\ \times \int ds^{N_T-N_1} \exp(-\beta U_{\mathrm{int},2}(s^{N_T-N_1}, (V_T - V_1))) \\ \times \left(\begin{array}{l} \delta_{i,1} \int ds^1_{\mathrm{frac}} \exp(-\beta U_{\mathrm{frac},1}(s_{\mathrm{frac}}, \lambda, V_1)) \\ + \delta_{i,2} \int ds^2_{\mathrm{frac}} \exp(-\beta U_{\mathrm{frac},2}(s_{\mathrm{frac}}, \lambda, (V_T - V_1))) \end{array} \right) \end{array} \right]$$

$$+ \frac{\frac{1}{Q_{\mathrm{CFCMC}}}}{\Lambda^{3(N_T+1)}\,(N_T)!} \sum_{N_1=0}^{N_T} \binom{N_T}{N_1} \int_0^1 d\lambda \int_0^{V_T} dV_1 \left[\begin{array}{l} {V_1}^{N_1+\delta_{i,1}} (V_T - V_1)^{N_T-N_1+\delta_{i,2}} \dfrac{\partial}{\partial V_T} \displaystyle\int ds^{N_1} \exp(-\beta U_{\mathrm{int},1}(s^{N_1}, V_1)) \\ \times \displaystyle\int ds^{N_T-N_1} \exp(-\beta U_{\mathrm{int},2}(s^{N_T-N_1}, (V_T - V_1))) \\ \times \left(\begin{array}{l} \delta_{i,1} \displaystyle\int ds^1_{\mathrm{frac}} \exp(-\beta U_{\mathrm{frac},1}(s_{\mathrm{frac}}, \lambda, V_1)) + \\ \delta_{i,2} \displaystyle\int ds^2_{\mathrm{frac}} \exp(-\beta U_{\mathrm{frac},2}(s_{\mathrm{frac}}, \lambda, (V_T - V_1))) \end{array} \right) \end{array} \right] \tag{S18}$$

The first expression in the right hand side of the Eq. S18 is related to the average density of box 2, in which the fractional molecule is also counted. The second expression in the right hand side of the Eq. S18, calculates the virial of all the pairs including the fractional molecule. Following the similar guidelines as for the conventional GE, the final expression for the thermodynamic pressure in the CFCMC GE is

$$P_{\mathrm{CFCMC},2} = k_B T \left(\frac{\partial \ln Q_{\mathrm{CFCMC}}}{\partial V_T} \right)_T = k_B T \left\langle \frac{N_2 + \delta_{i,2}}{V_2} \right\rangle_{\mathrm{CFCMC}} + \left\langle \frac{\sum_{a<b} f(r_{ab,2}) r_{ab,2}}{3V_2} \right\rangle_{\mathrm{CFCMC}} \tag{S19}$$

in which we have used $\langle ... \rangle_{\mathrm{CFCMC}}$ to denote ensemble averages in the CFCMC GE. By comparing Eqs. S14 and S19 it becomes clear that the thermodynamic pressures of the conventional GE and CFCMC GE are different, and therefore, one should be careful when calculating the coexistence pressure from CFCMC GE simulations.

Pressure Corresponding to the Conventional GE Computed in the CFCMC GE

Averages in the GE can be computed by running simulations in the CFCMC GE. One can write the following ensemble averages in CFCMC GE:

$$\left\langle \delta_{\lambda=0,i=1} \frac{1}{V_1} \right\rangle_{\text{CFCMC}} = \frac{1}{Q_{\text{CFCMC}}} \frac{1}{\Lambda^{3(N_T+1)}\,(N_T)!} \sum_{N_1=0}^{N_T} \binom{N_T}{N_1} \int_0^{V_T} dV_1 {V_1}^{N_1} (V_T - V_1)^{N_T - N_1} \times \int ds^{N_1} \exp(-\beta U_{\text{int},1}(s^{N_1}, V_1)) \int ds^{N_T - N_1} \exp(-\beta U_{\text{int},2}(s^{N_T-N_1}, (V_T - V_1))) \tag{S20}$$

$$\left\langle \delta_{\lambda=0,i=1} \frac{N_1}{{V_1}^2} \right\rangle_{\text{CFCMC}} = \frac{1}{Q_{\text{CFCMC}}} \frac{1}{\Lambda^{3(N_T+1)}\,(N_T)!} \sum_{N_1=0}^{N_T} \binom{N_T}{N_1} \int_0^{V_T} dV_1 {V_1}^{N_1} (V_T - V_1)^{N_T - N_1} \times \left(\frac{N_1}{V_1}\right) \int ds^{N_1} \exp(-\beta U_{\text{int},1}(s^{N_1}, V_1)) \int ds^{N_T - N_1} \exp(-\beta U_{\text{int},2}(s^{N_T-N_1}, (V_T - V_1))) \tag{S21}$$

Dividing Eq. S20 by Eq. S21, the term Q_{CFCMC} in the nominator and the denominator cancel, and we obtain

$$\frac{\left\langle \delta_{\lambda=0,i=1} \frac{N_1}{{V_1}^2} \right\rangle_{\text{CFCMC}}}{\left\langle \delta_{\lambda=0,i=1} \frac{1}{V_1} \right\rangle_{\text{CFCMC}}} = \frac{\sum_{N_1=0}^{N_T} \binom{N_T}{N_1} \int_0^{V_T} dV_1 {V_1}^{N_1} (V_T - V_1)^{N_T - N_1} \left(\frac{N_1}{V_1}\right) \left[\int ds^{N_1} \exp(-\beta U_{\text{int},1}(s^{N_1}, V_1)) \int ds^{N_T - N_1} \exp(-\beta U_{\text{int},2}(s^{N_T-N_1}, (V_T - V_1))) \right]}{\sum_{N_1=0}^{N_T} \binom{N_T}{N_1} \int_0^{V_T} dV_1 {V_1}^{N_1} (V_T - V_1)^{N_T - N_1} \left[\int ds^{N_1} \exp(-\beta U_{\text{int},1}(s^{N_1}, V_1)) \int ds^{N_T - N_1} \exp(-\beta U_{\text{int},2}(s^{N_T-N_1}, (V_T - V_1))) \right]} \tag{S22}$$

This yields the average density in the Gibbs ensemble

$$\frac{\left\langle \delta_{\lambda=0,i=1} \frac{N_1}{{V_1}^2} \right\rangle_{\text{CFCMC}}}{\left\langle \delta_{\lambda=0,i=1} \frac{1}{V_1} \right\rangle_{\text{CFCMC}}} = \left\langle \frac{N_1}{V_1} \right\rangle_{\text{GE}} \tag{S23}$$

In general, for any thermodynamic property X_j in box j, we can calculate $\langle X \rangle_{\text{GE}}$ from the CFCMC GE simulations. Repeating the same mathematical steps for any thermodynamic property property X, yields:

$$\langle X_j \rangle_{\text{GE}} = \frac{\left\langle \delta_{\lambda=0,i=j} \frac{X}{V_j} \right\rangle_{\text{CFCMC}}}{\left\langle \delta_{\lambda=0,i=j} \frac{1}{V_j} \right\rangle_{\text{CFCMC}}} \tag{S24}$$

We apply Eq. S24 to obtain the virial part of the pressure in the GE as well. Consequently, the pressure of box j corresponding to the conventional GE but computed in CFCMC GE becomes

$$P^*_{\text{GE},j} = k_B T \frac{\left\langle \delta_{\lambda=0,i=j} \frac{N_j}{{V^2}_j} \right\rangle_{\text{CFCMC}}}{\left\langle \delta_{\lambda=0,i=j} \frac{1}{V_j} \right\rangle_{\text{CFCMC}}} + \frac{\left\langle \delta_{\lambda=0,i=j} \frac{\sum\limits_{a<b} f_j(r_{ab,j}) r_{ab,j}}{3V_j^2} \right\rangle_{\text{CFCMC}}}{\left\langle \delta_{\lambda=0,i=1} \frac{1}{V_j} \right\rangle_{\text{CFCMC}}} \tag{S25}$$

which is identical to $P_{\text{GE},j}$.

References

1. Panagiotopoulos, A. Z.; Quirke, N.; Stapleton, M.; Tildesley, D. *Mol. Phys.* **1988**, *63*, 527–545.

2. Frenkel, D.; Smit, B. In *Understanding molecular simulation: from algorithms to applications*; Frenkel, D., Michael, K., Michele, P., Smit, B., Eds.; Academic Press: San Diego, California, 2002; Vol. 1.

3. Flanders, H. *Am. Math. Monthly* **1973**, *80*, 615–627.

4. Allen, M. P.; Tildesley, D. J. *Computer simulation of liquids*; Oxford University Press: New York, 1989.

5. Poursaeidesfahani, A.; Torres-Knoop, A.; Dubbeldam, D.; Vlugt, T. J. H. *J. Chem. Theo. Comp.* **2016**, *12*, 1481–1490.